Polymer Chemistry

PAPER

View Article Online
View Journal | View Issue

Check for updates

Cite this: *Polym. Chem.*, 2017, **8**, 4811

Phenyl acrylate is a versatile monomer for the synthesis of acrylic diblock copolymer nano-objects *via* polymerization-induced self-assembly†

S. L. Canning, V. J. Cunningham, L. P. D. Ratcliffe and S. P. Armes *

Over the last decade or so, polymerization-induced self-assembly (PISA) has become widely recognized as a versatile technique for the rational synthesis of diblock copolymer nano-objects in the form of concentrated dispersions. However, there are relatively few examples of acrylic-based PISA formulations in the literature, partly because such copolymers typically possess relatively low glass transition temperatures (T_g) that preclude morphological characterization by transmission electron microscopy. To address this problem, we have selected phenyl acrylate (PhA) as a model monomer to generate the solvophobic block in three PISA formulations using reversible addition–fragmentation chain transfer (RAFT) polymerization. Thus, a poly(dimethyl acrylamide)-based chain transfer agent (CTA) is chain-extended using PhA *via* RAFT aqueous emulsion polymerization to produce a series of well-defined sterically-stabilized spheres whose mean diameter can be readily adjusted from 38 nm to 188 nm by varying the target degree of polymerization (DP). In contrast, RAFT alcoholic dispersion polymerization of PhA using a poly(acrylic acid) CTA leads to an evolution of copolymer morphology from spheres to worms to lamellae and finally vesicles as the target DP of the structure-directing PPhA block is increased. Similarly, RAFT dispersion polymerization of PhA in *n*-heptane also produces spheres, worms or vesicles depending on the target DP of the PPhA block. ^{1}H NMR studies indicate that >98% PhA conversion is achieved in all cases, while GPC analysis indicates high blocking efficiencies. However, relatively broad molecular weight distributions are observed (M_w/M_n = 1.37 to 2.48), which suggests extensive chain transfer to polymer in such PISA syntheses, particularly in the case of the RAFT aqueous emulsion polymerization formulation. Nevertheless, the relatively high T_g of PPhA (50 °C) enables characterization of the various copolymer morphologies using conventional TEM.

Received 12th July 2017,
Accepted 17th July 2017

DOI: 10.1039/c7py01161j

rsc.li/polymers

Open Access Article. Published on 25 July 2017. Downloaded on 3/28/2024 2:51:24 PM.
This article is licensed under a Creative Commons Attribution 3.0 Unported Licence.

Introduction

AB diblock copolymers are well-known to self-assemble into well-defined micelles in a solvent that is selective for one of the two blocks.[1–9] In principle, a wide range of morphologies can be obtained depending on the relative volume fractions of each block.[10,11] Traditionally, this self-assembly involves some form of post-polymerization processing (*e.g.* a pH switch, a solvent switch or thin film rehydration) that is conducted at high dilution and typically at rather low final copolymer concentrations (<1% w/w). With the advent of controlled radical polymerization (CRP) techniques such as nitroxide-mediated polymerization (NMP),[12] atom transfer radical polymerization (ATRP)[13,14] and reversible addition–fragmentation chain transfer (RAFT) polymerization,[15] polymerization-induced self-assembly (PISA) has recently become established as a versatile platform technology for the rational synthesis of diblock copolymer nano-objects at high solids, which eliminates the requirement for further processing steps.[16–19]

In practice, most of the PISA formulations reported in the literature are based on RAFT polymerization.[16–22] Robust RAFT dispersion polymerization formulations have been developed for water,[16,19,20,23–32] lower alcohols[17,33–40] and non-polar solvents[17,41–45] while RAFT aqueous emulsion polymerization has also been thoroughly explored.[46–52] However, the vast majority of PISA syntheses reported in the literature involve polymerization of methacrylic or styrenic monomers rather than acrylic monomers, despite the commercial importance of the latter monomer class. Acrylic polymers typically exhibit glass transition temperatures (T_g) well below ambient temperature, which makes them very useful for paints and coatings[53]

Department of Chemistry, University of Sheffield, Dainton Building, Brook Hill, Sheffield, South Yorkshire S3 7HF, UK. E-mail: s.p.armes@sheffield.ac.uk

†Electronic supplementary information (ESI) available: Assigned ^{1}H NMR spectra of the macro-CTA and diblock copolymer in each of the three solvent systems. See DOI: 10.1039/c7py01161j

Open Access Article. Published on 25 July 2017. Downloaded on 3/28/2024 2:51:24 PM.
This article is licensed under a Creative Commons Attribution 3.0 Unported Licence.

and also adhesion applications.[54] Unfortunately, this makes the examination of copolymer morphology *via* conventional transmission electron microscopy (TEM) rather problematic, and such characterization is usually an important component of most PISA studies. In principle, cryo-TEM can be utilized instead, but in practice this technique is not widely available and relatively expensive; moreover, appropriate sample preparation protocols are not well-developed for imaging non-aqueous formulations.

Chain transfer to polymer is well known for the polymerization of acrylic monomers.[55–57] This side reaction leads to branching and hence significant broadening of the molecular weight distribution (MWD), although this can be mitigated to some extent by using CRP techniques.[58,59] This problem may explain why relatively few acrylic-based PISA formulations have been reported in the literature.[45,60–67] These include syntheses conducted in either water,[60,61,64,65] *n*-alkanes[45,63,66] or ethanol/water mixtures.[62,67] For example, Ratcliffe *et al.* recently chain-extended a poly(lauryl acrylate) (PLA) macromolecular chain transfer agent (macro-CTA) using benzyl acrylate (BzA) to produce PLA-PBzA diblock copolymer nano-objects in either *n*-heptane, *n*-dodecane or iso-hexadecane.[66] By varying the target DP of the PBzA core-forming block, pure phases of spheres, worms and vesicles could be produced. However, relatively broad molecular weight distributions were observed, with M_w/M_n values ranging from 1.53 to 1.67 when targeting PBzA DPs of 55–90 at 25% w/w solids. Moreover, the relatively low T_g of PBzA (6 °C) prevented characterization of the nano-object morphology by conventional TEM, so cryo-TEM was utilized instead.[66]

In principle, one solution to this imaging problem is to simply select an acrylic polymer with a relatively high T_g. In practice, very few acrylic monomers are suitable in this regard. Nevertheless, this approach was recently reported by Tan *et al.*, who polymerized isobornyl acrylate (IBOA; T_g of PIBOA = 94 °C) using a poly(ethylene glycol)-based macro-CTA.[67] This PISA synthesis was conducted in an 85/15 ethanol/water mixture at 40 °C using visible light to initiate the polymerization. High conversions (>95%) were obtained within 30 min and relatively narrow molecular weight distributions were reported (*e.g.* M_w/M_n = 1.26 when targeting a PIBOA DP of 150). However, diblock copolymers were typically contaminated with approximately 10–20% unreacted macro-CTA. Nevertheless, either spheres, worms or vesicles could be produced depending on the PISA synthesis conditions, as judged by conventional TEM studies.

In the present work, we have chosen to study phenyl acrylate (PhA) as a model acrylic monomer in the context of three PISA formulations. Poly(phenyl acrylate) (PPhA) has a relatively high T_g of 50 °C,[68] which should be sufficient to enable copolymer morphology studies using conventional TEM. To evaluate the versatility of this new monomer, we studied its use in RAFT aqueous emulsion polymerization, RAFT alcoholic dispersion polymerization and RAFT dispersion polymerization in *n*-alkanes using suitable macro-CTAs as the steric stabilizer block.

Experimental section

Materials

Lauryl acrylate (LA, 98%) was purchased from Tokyo Chemical Industry UK Ltd. Phenyl acrylate (PhA, 97%) was purchased from Alfa Aesar (UK). Both monomers were used as received. 2-(Dodecylthiocarbonothioylthio)-2-methylpropionic acid (DDMAT, 98%), dimethyl acrylamide (DMAC, 99%), acrylic acid (AA, 99%), potassium persulfate (KPS, 99%), L-ascorbic acid (AscAc, 99%) and azoisobutyronitrile (AIBN, 98%) were purchased from Sigma Aldrich (UK) and were used as received. *tert*-Butyl peroxy-2-ethylhexanoate (T21S) was purchased from AkzoNobel (The Netherlands). Dimethyl sulfoxide-d_6, $CDCl_3$ and DMF-d_7 were purchased from Goss Scientific Instruments Ltd (Cheshire, UK). All other solvents were purchased from Fisher Scientific (Loughborough, UK) and were used as received. Deionized water was used for all aqueous PISA formulations.

Synthesis of $PDMAC_{53}$ macro-CTA by RAFT solution polymerization

A typical protocol for the synthesis of a $PDMAC_{53}$ macro-CTA was as follows. DMAC monomer (0.141 mol, 14.021 g), DDMAT RAFT agent (2.57 mmol, 0.9376 g) and dioxane (0.397 mol, 35.00 g, corresponding to a 30% w/w solution) were added to a round-bottomed flask in order to target a mean DP of 55. AIBN initiator (0.257 mmol, 0.0422 g, CTA/AIBN molar ratio = 10.0) was added to this mixture, and the resulting yellow solution was cooled by immersion in an ice bath while sparging with N_2 gas for 30 min, before the sealed flask was placed in an oil bath set at 70 °C. After 35 min, the polymerization was quenched by immersion of the reaction flask in ice, followed by exposure to air. The final DMAC conversion was determined to be 92% by ^{1}H NMR spectroscopy. The crude PDMAC macro-CTA was then precipitated twice into a ten-fold excess of diethyl ether to remove unreacted DMAC and other residual reagents before being dried in a vacuum oven overnight at 20 °C. ^{1}H NMR analysis indicated a mean DP of 53 for the final purified PDMAC macro-CTA, which suggests a CTA efficiency of 95%. THF GPC analysis of $PDMAC_{53}$ macro-CTA indicated M_n and M_w/M_n values of 5400 g mol^{-1} and 1.08, respectively.

Synthesis of $PDMAC_{53}$-$PPhA_x$ diblock copolymer nano-objects by RAFT aqueous emulsion polymerization

A typical protocol for the synthesis of $PDMAC_{53}$-$PPhA_{100}$ diblock copolymer was as follows: $PDMAC_{53}$ macro-CTA (0.200 g, 0.0356 mmol), KPS (1.90 mg, 0.007 mmol; CTA/initiator molar ratio = 5.0) and water (2.192 g, corresponding to a 25% w/w aqueous solution) were weighed into a 25 mL round-bottom flask and purged with nitrogen for 30 min. Ascorbic acid (2.0 mg, 16 μmol, CTA/initiator molar ratio = 5.0; prepared as a 10% w/w aqueous solution) was degassed separately with nitrogen for 30 min prior to addition to the aqueous solution in the reaction flask. Phenyl acrylate (0.527 g, 3.56 mmol) was also degassed separately with nitrogen for

 This journal is © The Royal Society of Chemistry 2017

Open Access Article. Published on 25 July 2017. Downloaded on 3/28/2024 2:51:24 PM.
This article is licensed under a Creative Commons Attribution 3.0 Unported Licence.

30 min and added last to the reaction flask, which was then sealed and immersed in an oil bath set at 30 °C. The reaction mixture was stirred for 4.5 h to ensure high monomer conversion (>99% by ^{1}H NMR analysis) and subsequently quenched by cooling to 20 °C, followed by exposure to air. DMF GPC analysis of $PDMAC_{53}$-$PPhA_{100}$ indicated M_n and M_w/M_n values of 18 400 g mol^{-1} and 2.10, respectively.

Synthesis of PAA_{26} macro-CTA

A typical protocol for the synthesis of a PAA_{26} macro-CTA was as follows. AA monomer (0.080 mol, 6.000 g), DDMAT RAFT agent (2.78 mmol, 1.011 g), and ethanol (0.081 mol, 7.102 g, corresponding to a 50% w/w solution) were added to a round-bottomed flask in order to target a mean DP of 30. AIBN initiator (0.56 mmol, 0.091 g, CTA/AIBN molar ratio = 5.0) was added to this mixture, and the resulting yellow solution was cooled in an ice bath while sparging with N_2 gas for 30 min, before the sealed flask was immersed in an oil bath set at 60 °C. After 150 min, the polymerization was quenched by immersion of the reaction flask in an ice bath, followed by exposure to air. ^{1}H NMR spectroscopy indicated a final AA conversion of 85%. The crude polymer was then precipitated twice into a ten-fold excess of diethyl ether before being dried in a vacuum oven at 20 °C. ^{1}H NMR analysis indicated a mean DP of 26 for this PAA macro-CTA, which suggests a CTA efficiency of 98%. THF GPC analysis of this PAA_{26} macro-CTA indicated M_n and M_w/M_n values of 3400 g mol^{-1} and 1.07, respectively.

Synthesis of PAA_{26}-$PPhA_x$ diblock copolymers by RAFT alcoholic dispersion polymerization

A typical protocol for the synthesis of PAA_{26}-$PPhA_{50}$ diblock copolymer nano-objects was as follows: PAA_{26} macro-CTA (0.080 g, 0.035 mmol) was added to a glass vial, followed by PhA monomer (0.265 g, 1.787 mmol) and ethanol (1.038 g, corresponding to a 25% w/w solution). AIBN initiator was then added (1.20 mg, 7.15 μmol, CTA/AIBN molar ratio = 5.0). This flask was cooled using an ice bath, and the solution was sparged with N_2 gas for 25 min. The flask was then sealed and immersed in an oil bath set at 70 °C. The reaction mixture was stirred for 16 h to ensure high monomer conversion (>99% by ^{1}H NMR analysis) and subsequently quenched by cooling followed by exposure to air. THF GPC analysis of PAA_{26}-$PPhA_{50}$ indicated M_n and M_w/M_n values of 8100 g mol^{-1} and 1.68, respectively.

Synthesis of PLA_{14} macro-CTA

A typical protocol for the synthesis of a PLA_{14} macro-CTA was as follows. LA monomer (0.32 mol, 76.92 g), DDMAT RAFT agent (12.8 mmol, 4.67 g), and acetone (1.41 mol, 82.0 g) were added to a round-bottomed flask in order to target a mean DP of 25. AIBN initiator (2.56 mmol, 0.420 g, CTA/AIBN molar ratio = 5.0) was added to this mixture, and the resulting yellow solution was cooled in an ice bath while sparging with N_2 gas for 30 min, before the sealed flask was immersed in an oil bath set at 70 °C. After 125 min, the polymerization was quenched by immersion of the reaction flask in ice, followed by exposure to air. A final LA conversion of 55% was determined by ^{1}H NMR spectroscopy. This crude polymer solution was then precipitated twice into a ten-fold excess of cold methanol and washed in further methanol before being dried under vacuum for 72 h at 20 °C. ^{1}H NMR analysis indicated a mean DP of 14 for this PLA macro-CTA, which suggests a CTA efficiency of 98%. THF GPC analysis indicated M_n and M_w/M_n values of 3700 g mol^{-1} and 1.12, respectively.

Synthesis of PLA_{14}-$PPhA_x$ diblock copolymers by RAFT dispersion polymerization in *n*-alkanes

A typical protocol for the synthesis of PLA_{14}-$PPhA_{80}$ diblock copolymer nano-objects was as follows: PLA_{14} macro-CTA (0.180 g, 0.05 mmol) was added to a 14 mL glass vial, followed by PhA monomer (0.572 g, 3.86 mmol) and *n*-heptane (2.05 g). T21S initiator was then added (2.08 mg, 0.01 mmol; CTA/T21S molar ratio = 5.0), as a 1.0% solution in *n*-heptane to make up a 25% w/w solution. This flask was cooled using an ice bath, and the solution was sparged with N_2 gas for 20 min. The flask was then sealed and immersed in an oil bath set at 80 °C. The reaction mixture was stirred for 16 h to ensure high monomer conversion (99% according to ^{1}H NMR analysis) and subsequently quenched by cooling to 20 °C, followed by exposure to air. THF GPC analysis of PLA_{14}-$PPhA_{80}$ indicated M_n and M_w/M_n values of 13 800 g mol^{-1} and 1.44, respectively.

Copolymer characterization

^{1}H NMR spectroscopy

All ^{1}H NMR spectra were recorded on a 400 MHz Bruker Avance-400 spectrometer using DMF-d_7 ($PDMAC_{53}$-$PPhA_x$), dimethyl sulfoxide-d_6 (PAA_{26}-$PPhA_x$) and $CDCl_3$ (PLA_{14}-$PPhA_x$) as deuterated solvents.

Gel permeation chromatography (GPC)

Molecular weight distributions of the PAA_{26}-$PPhA_x$ and PLA_{14}-$PPhA_x$ diblock copolymers were assessed by GPC using THF eluent. For the former series of copolymers, such analysis required exhaustive methylation of the carboxylic acid groups in the PAA block with excess trimethylsilyldiazomethane to prevent column adsorption. The GPC set-up consisted of two 5 μm Mixed C columns (30 cm) and a WellChrom K-2301 refractive index detector operating at 950 ± 30 nm. The mobile phase contained 2.0% v/v triethylamine and 0.05% w/v butylhydroxytoluene (BHT) with a toluene flow rate marker and the flow rate was fixed at 1.0 mL min^{-1}. Copolymer solutions (1.0% w/v) were prepared in THF. A series of ten near-monodisperse poly(methyl methacrylate) standards (M_p values ranging from 1280 to 330 000 g mol^{-1}) were used for calibration. Data were analyzed using Agilent GPC/SEC software (version 1.2). The molecular weights and dispersities of the $PDMAC_{53}$-$PPhA_x$ diblock copolymers were determined by GPC using DMF eluent at 60 °C. The GPC set-up consisted of two Polymer Laboratories PL gel 5 μm Mixed C columns connected in series to an Agilent 1260 Infinity GPC/SEC system with refractive index and variable wavelength detectors and autosampler. The mobile phase was HPLC-grade DMF containing 10 mM LiBr with a flow rate of 1.0 mL min^{-1}. Copolymer solutions

Open Access Article. Published on 25 July 2017. Downloaded on 3/28/2024 2:51:24 PM.
This article is licensed under a Creative Commons Attribution 3.0 Unported Licence.

(1.0% w/v) were prepared in DMF. Ten near-monodisperse PMMA standards (M_n = 625 to 618 000 g mol^{-1}) were used for calibration. Data were analyzed using Agilent GPC/SEC software (version 1.2).

Dynamic light scattering (DLS)

The intensity-average hydrodynamic diameter of each batch of diblock copolymer nanoparticles was determined from the Stokes–Einstein equation using a Malvern Instruments Zetasizer NanoZS instrument. Dilute (0.20% w/w) copolymer dispersions were analyzed and data were averaged over three consecutive runs. Measurements were made at 25 °C and the scattered light was detected at an angle of 173°.

Transmission electron microscopy (TEM)

Copper/palladium TEM grids (Agar Scientific, UK) were coated in-house to yield a thin film of amorphous carbon. For the PDMAC$_{53}$-PPhA$_x$ and PAA$_{26}$-PPhA$_x$ samples, the grids were then subjected to a glow discharge for 30 s to create a hydrophilic surface. Individual samples (0.20% w/w dispersion, 10.0 μL) were placed on the freshly-treated grids for 1 min and then blotted with filter paper to remove excess solution. To stain the colloidal aggregates, uranyl formate (9.0 μL of a 0.75% w/w solution) was absorbed onto the sample-loaded grid for 20 s and then carefully blotted to remove excess stain. The grids were then dried using a vacuum hose. For the PLA$_{14}$-PPhA$_x$ samples, each dispersion (0.20% w/w, 11 μL) was placed on a grid for 1 min and then blotted with filter paper to remove excess solution. To stain the deposited nanoparticles, each grid was exposed to ruthenium(IV) oxide vapor for 7 min at 20 °C prior to analysis.[41] This heavy metal compound acted as a positive stain to improve electron contrast. The ruthenium (IV) oxide was prepared as follows: ruthenium(II) oxide (0.30 g) was added to water (50 g) to form a black slurry; addition of sodium periodate (2.0 g) with stirring produced a yellow solution of ruthenium(IV) oxide within 1 min. Imaging of all grids was performed using a Philips CM100 instrument operating at 100 kV equipped with a Gatan 1 k CCD camera.

Results and discussion

One major obstacle to the more widespread use of acrylates in PISA formulations are the relatively low T_g values exhibited by such polymers. In contrast, PPhA has a T_g of 50 °C, which is comparable to that of poly(2-hydroxypropyl methacrylate) or poly(benzyl methacrylate).[69] Many high-quality TEM images have been reported for PISA formulations based on such methacrylic core-forming blocks,[33,34,46,70] so it was considered likely that similar results could be obtained for PPhA. To exemplify the versatility offered by the use of phenyl acrylate, we devised three new acrylic-based RAFT-mediated PISA formulations based on this monomer (see Fig. 1). Thus RAFT aqueous emulsion polymerization of PhA utilized a PDMAC$_{53}$ macro-CTA, while RAFT dispersion polymerization of PhA in ethanol used PAA$_{26}$ as a stabilizer block. Finally, RAFT dispersion polymerizations conducted in *n*-heptane were conducted using a PLA$_{14}$ macro-CTA. Each of these three PISA formulations is discussed in turn below.

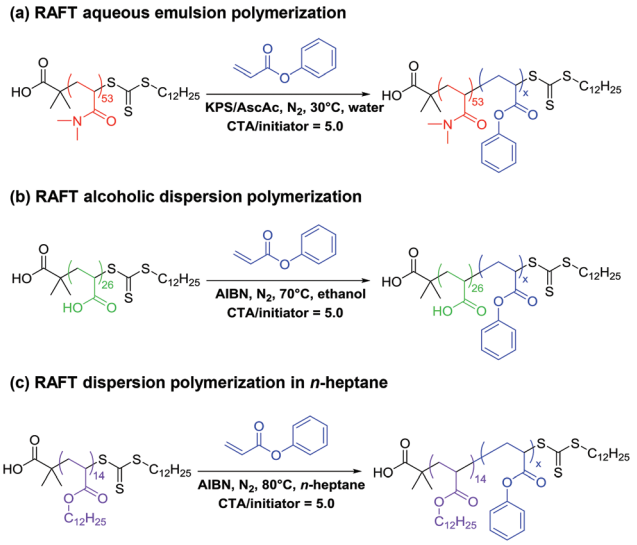


Fig. 1 Polymerization of phenyl acrylate *via* three different PISA formulations: (a) RAFT aqueous emulsion polymerization at 30 °C, (b) RAFT alcoholic dispersion polymerization in ethanol at 70 °C and (c) RAFT dispersion polymerization in *n*-heptane at 80 °C.

RAFT aqueous emulsion polymerization of phenyl acrylate using PDMAC$_{53}$ stabilizer

The PDMAC$_{53}$ macro-CTA was synthesized by RAFT solution polymerization in dioxane using 2-(dodecylthiocarbonothioylthio)-2-methylpropionic acid (DDMAT) as the RAFT agent, as this CTA is well-suited for the controlled polymerization of both acrylic and acrylamide-based monomers.[30,66] A low-temperature synthesis protocol was selected for the synthesis of PDMAC$_{53}$-PPhA$_x$ diblock copolymer nanoparticles *via* RAFT aqueous emulsion polymerization in an attempt to minimize chain transfer to polymer, which is well-known for the polymerization of acrylic monomers.[55–59] This problem leads to broadening of the molecular weight distribution *via* long-chain branching. Thus a redox initiator system comprising KPS and ascorbic acid was selected to enable polymerizations to be conducted at 30 °C.[65]

A series of PDMAC$_{53}$-PPhA$_x$ copolymers was prepared with a target PPhA DP (x) ranging from 50 to 500, see Table 1. High conversions were obtained in all cases (>98% for x = 50–500; entries 1–7). DMF GPC analysis indicated relatively high blocking efficiencies, with the copolymer molecular weight increasing monotonically with target core-forming block DP, as expected. However, M_w/M_n values ranged from 1.85 to 2.48 with no apparent trend between DP and dispersity (Fig. 2). This is perhaps surprising given the relatively low reaction temperature selected for these PISA syntheses, and this point will be considered later.

Spherical nanoparticles were produced in all cases, as confirmed by both DLS analysis and TEM (Fig. 3). This kinetically-

 This journal is © The Royal Society of Chemistry 2017

Open Access Article. Published on 25 July 2017. Downloaded on 3/28/2024 2:51:24 PM.
This article is licensed under a Creative Commons Attribution 3.0 Unported Licence.

Table 1 Summary of monomer conversions, GPC molecular weight data, DLS particle diameters and TEM morphologies obtained for a series of $PDMAC_{53}$-$PPhA_x$ diblock copolymers prepared *via* RAFT aqueous emulsion polymerization at 30 °C[a]

Entry no.	Target diblock composition	Conversion[b]/%	DMF GPC[c] M_n	DMF GPC[c] M_w/M_n	DLS diameter[d]/nm	TEM morphology
1	$PDMAC_{53}$-$PPhA_{50}$	>99	12 400	1.85	38 (0.27)	Spheres
2	$PDMAC_{53}$-$PPhA_{100}$	>99	18 400	2.10	54 (0.12)	Spheres
3	$PDMAC_{53}$-$PPhA_{150}$	>99	24 700	2.19	68 (0.12)	Spheres
4	$PDMAC_{53}$-$PPhA_{200}$	>99	30 600	2.22	79 (0.07)	Spheres
5	$PDMAC_{53}$-$PPhA_{300}$	>99	41 200	2.48	105 (0.08)	Spheres
6	$PDMAC_{53}$-$PPhA_{400}$	98	53 300	2.43	133 (0.08)	Spheres
7	$PDMAC_{53}$-$PPhA_{500}$	99	61 400	2.06	188 (0.21)	Spheres

[a] Conditions: [macro-CTA] : [initiator] molar ratio = 5.0; copolymer concentration = 25% w/w. [b] Monomer conversion determined by ^{1}H NMR spectroscopy in DMF-d_7. [c] Refractive index detector, calibrated with a series of near-monodisperse poly(methyl methacrylate) standards. [d] DLS: intensity-average diameters were calculated using cumulants analysis software provided by the manufacturer (Malvern Instruments, UK). The numbers in brackets denote the polydispersity in the particle diameter.

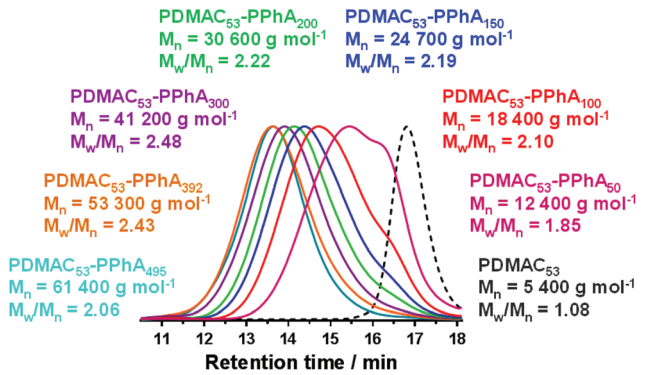


Fig. 2 DMF GPC curves for $PDMAC_{53}$-$PPhA_x$ diblock copolymers prepared at 25% w/w solids *via* RAFT aqueous emulsion polymerization of PhA at 30 °C. M_n values are expressed relative to a series of near-monodisperse poly(methyl methacrylate) calibration standards.

trapped morphology has been reported for many RAFT aqueous emulsion polymerization syntheses,[46,48,61,71–76] but this phenomenon is not properly understood. However, it is perhaps noteworthy that the relatively few such PISA formulations yielding non-spherical nano-objects employed either (i) statistical copolymer macro-CTAs comprising a 1 : 1 molar ratio of (meth)acrylic acid and oligo(ethylene glycol) (meth) acrylate,[51,52,77,78] (ii) copolymer macro-CTAs comprising a poly (*N*-acryloylmorpholine) (PNAM) block with a few poly(ethylene glycol) acrylate (PEGA) units with varying position within the polymer chain or (iii) a monomer exhibiting a relatively high aqueous solubility (*e.g.* 4-hydroxybutyl methacrylate).[47] Nevertheless, in the present study the PISA mechanism provided good control over the particle size, with a monotonic increase in the intensity-average particle diameter being observed when targeting core-forming DPs ranging from 50 to 500 (see Fig. 3).

RAFT dispersion polymerization of phenyl acrylate in ethanol

It is now well-established that RAFT alcoholic dispersion polymerization normally enables access to worms or vesicles when targeting longer solvophobic blocks, provided that the steric stabilizer block is sufficiently short to allow efficient sphere-sphere fusion to occur on the time scale of the PISA synthesis.[16–18,20,23,25,28,79–81] Accordingly, for the RAFT dispersion polymerization of PhA in ethanol, a PAA macro-CTA with a mean DP of 26 was synthesized *via* RAFT solution polymerization in ethanol using DDMAT as the RAFT agent. Following exhaustive methylation with excess trimethylsilyldiazomethane, THF GPC analysis indicated an M_w/M_n of 1.07, suggesting good RAFT control. This PAA_{26} macro-CTA was then used for the polymerization of PhA in ethanol at 70 °C using AIBN initiator. For such PISA formulations, higher copolymer concentrations (*e.g.* 25% w/w solids, as used herein) favor the production of pure (rather than mixed) phases.

Table 2 summarizes the target PAA_{26}-$PPhA_x$ compositions, with x ranging from 30 to 300. Analysis by ^{1}H NMR indicated that the final monomer conversion was high (>98%) in all cases. Following exhaustive methylation of the carboxylic acid residues in the PAA block, THF GPC analysis indicated marginally narrower molecular weight distributions compared to those obtained for the series of $PDMAC_{53}$-$PPhA_x$ diblock copolymers prepared by RAFT aqueous emulsion polymerization (compare Tables 1 and 2). Although relatively high blocking efficiencies were obtained, the molecular weight distributions were again rather broad compared to those typically obtained for PISA syntheses based on methacrylic diblock copolymers.[16–22] For this second series of all-acrylic copolymers, increasing the target DP of the core-forming block led to a gradual increase in dispersity (see Fig. 4). The weak high molecular weight shoulder is similar to that previously reported by Ratcliffe and co-workers[66] for PLA_{14}-$PBzA_x$ syntheses conducted *via* PISA in non-polar solvents; this feature is postulated to be either the result of chain transfer to polymer or possibly owing to termination by combination.

An evolution in copolymer morphology occurs when targeting higher PPhA DPs for this PISA system. Thus a relatively transparent dispersion is obtained at a PPhA DP of 30, with DLS and TEM studies indicating the presence of relatively small spheres with an intensity-average diameter of 24 nm. As the PPhA DP is increased to 50, a pure worm phase is obtained

Open Access Article. Published on 25 July 2017. Downloaded on 3/28/2024 2:51:24 PM.
This article is licensed under a Creative Commons Attribution 3.0 Unported Licence.

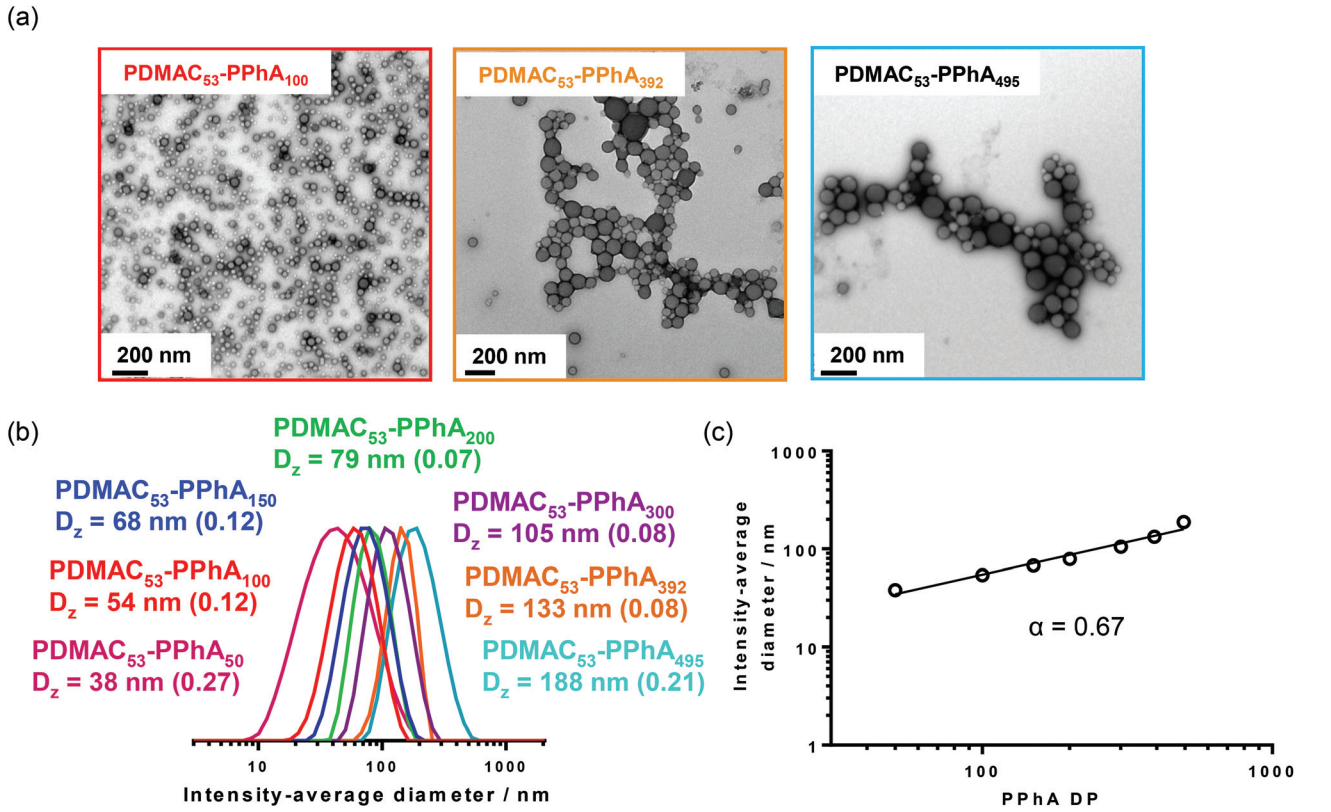


Fig. 3 A series of PDMAC$_{53}$-PPhA$_x$ diblock copolymers prepared at 25% w/w solids *via* RAFT aqueous emulsion polymerization of PhA conducted at 30 °C using a PDMAC$_{53}$ macro-CTA. (a) Selected TEM images showing well-defined spherical nanoparticles; (b) corresponding DLS intensity-average size distributions and (c) the relationship between the DP of the core-forming PPhA block and the intensity-average DLS diameter, where α is the scaling factor.

Table 2 Summary of monomer conversions, GPC molecular weight data, DLS particle diameters, and copolymer morphologies obtained for a series of PAA$_{26}$-PPhA$_x$ diblock copolymers synthesized *via* RAFT dispersion polymerization of phenyl acrylate in ethanol at 70 °C[a]

			GPC data[c]			
Entry no.	Target diblock composition	Monomer conversion[b]/%	M_n	M_w/M_n	DLS diameter[d]/nm	TEM morphology
1	PAA$_{26}$-PPhA$_{30}$	98	7200	1.45	24 (0.22)	Spheres
2	PAA$_{26}$-PPhA$_{50}$	>99	8100	1.68	231 (0.38)	Worms
3	PAA$_{26}$-PPhA$_{75}$	99	14 500	1.50	2800 (0.88)	Lamellae
4	PAA$_{26}$-PPhA$_{100}$	98	12 300	1.77	1300 (0.28)	Lamellae + vesicles
5	PAA$_{26}$-PPhA$_{150}$	98	12 200	2.13	970 (0.09)	Vesicles
6	PAA$_{26}$-PPhA$_{300}$	98	41 200	2.48	3400 (0.95)	Precipitate

[a] Conditions: [macro-CTA] : [initiator] molar ratio = 5.0; copolymer concentration = 25% w/w. [b] Monomer conversion determined by ^{1}H NMR spectroscopy in DMSO-d$_6$. [c] Determined by THF GPC (refractive index detector, calibrated using a series of poly(methyl methacrylate) standards). [d] Intensity-average diameters were calculated using cumulants analysis software provided by the manufacturer (Malvern Instruments, UK). The numbers in brackets denote the polydispersity in the particle diameter.

in the form of a transparent soft gel. At a PPhA DP of 74, a transparent brittle gel was produced with DLS studies indicating a large sphere-equivalent diameter (>2 μm) and relatively high polydispersity (0.88). TEM studies suggest that this is actually a lamellar phase, with large stacked 'sheets'. Similar lamellae have been reported by Yang *et al.*,[26,82] who also utilized a RAFT dispersion polymerization formulation comprising ethanol plus a co-solvent (either dioxane or methyl ethyl ketone). In these two earlier studies the formation of such a lamellar morphology was rationalized in terms of the relatively high T_g (219 °C) of the poly(styrene-*alt*-*N*-phenylmaleimide) core-forming block impeding vesicle formation. However, the present study suggests that other as-yet-unidentified factors may be responsible for the formation of such lamellar morphologies.

Increasing the PPhA DP up to 98 produced a mixed phase comprising lamellae and vesicles, suggesting that the lamellar

 This journal is © The Royal Society of Chemistry 2017

Open Access Article. Published on 25 July 2017. Downloaded on 3/28/2024 2:51:24 PM.
This article is licensed under a Creative Commons Attribution 3.0 Unported Licence.

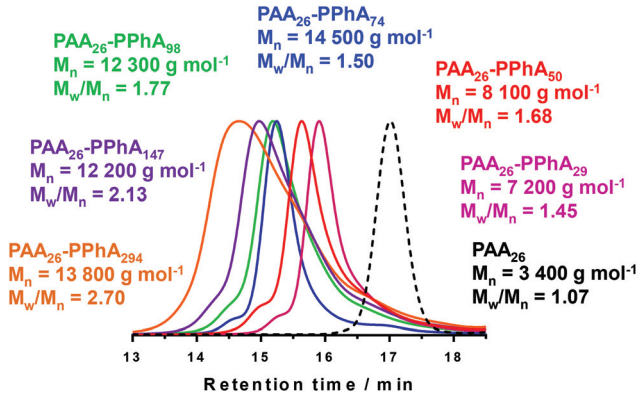


Fig. 4 THF GPC curves obtained for PAA_{26}-$PPhA_x$ diblock copolymers prepared at 25% w/w solids *via* RAFT alcoholic dispersion polymerization of PhA at 70 °C. Molecular weight data are expressed relative to a series of near-monodisperse poly(methyl methacrylate) calibration standards.

sheets are sufficiently deformable to enable vesicle formation to occur *via* 'wrap up'. The visual appearance of PAA_{26}-$PPhA_{147}$ (entry 6 in Table 2) was a turbid free-flowing dispersion, which is characteristic of vesicles in the PISA literature.[66,81,83,84] TEM studies confirmed this morphology, with some evidence for the presence of oligolamellar vesicles (see Fig. 5). Finally, a precipitate phase comprising polydisperse particles of approximately 6 μm was observed when targeting PAA_{26}-$PPhA_{300}$ (see entry 6 in Table 2 and Fig. 5). Given the highly asymmetric nature of these latter diblock copolymer chains, it seems likely that 'vesicle death' has occurred in this case. As reported by Warren *et al.*,[27] the overall vesicle diameter is conserved during PISA. Thus, as the membrane thickens, the volume of the vesicle lumen must shrink. This leads to sterically congested stabilizer chains within the inner leaflet, which ultimately leads to vesicle destabilization. Strong evidence to support this upper limit constraint on vesicle growth was recently confirmed by Derry *et al.*[85] *via in situ* synchrotron SAXS studies. Given that 'vesicle death' has been observed for PISA syntheses conducted in both water and mineral oil, this suggests a *generic* mechanism that is hence also likely to apply to the current RAFT alcoholic dispersion polymerization formulation.

RAFT dispersion polymerization of phenyl acrylate in *n*-heptane

A wide range of copolymer morphologies could also be accessed *via* RAFT dispersion polymerization of PhA in *n*-heptane at 80 °C. These syntheses were conducted using a PLA_{14} macro-CTA at 25% w/w solids to enable direct comparison with the other two PISA formulations. Again, a series of PLA_{14}-$PPhA_x$ diblock copolymers were produced by systematically varying the PPhA target DP (see Table 3). According to ^{1}H NMR studies, high conversions (>98%) were obtained in each case.

As expected, the apparent GPC M_n for this series of diblock copolymers increased with increasing PPhA DP. Moreover, THF GPC analysis suggested high blocking efficiencies, with

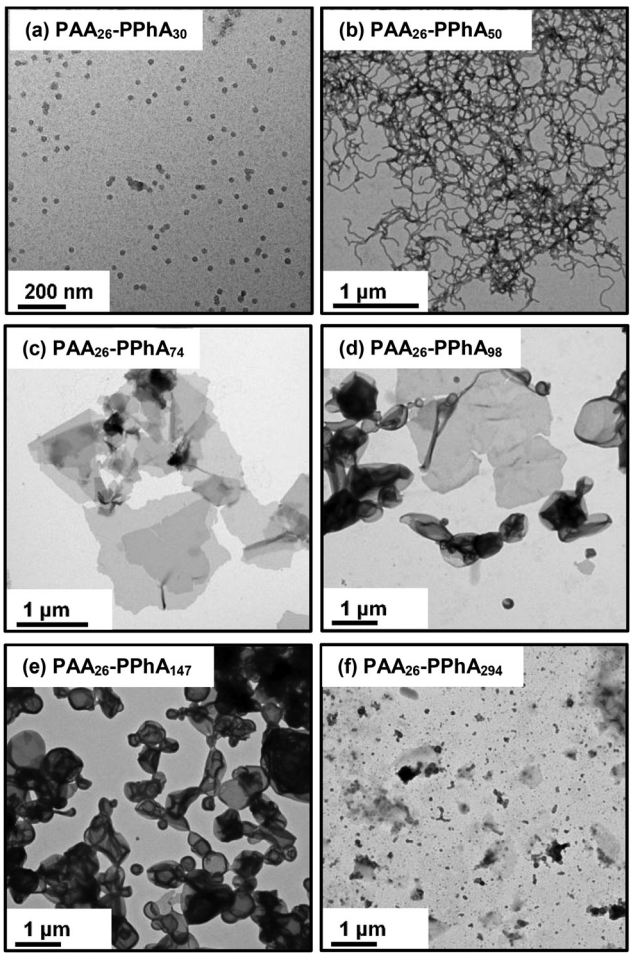


Fig. 5 PAA_{26}-$PPhA_x$ diblock copolymers prepared at 25% w/w solids by RAFT alcoholic dispersion polymerization of PhA at 70 °C: selected TEM images showing the evolution in copolymer morphology to form (a) spheres, (b) worms, (c) lamellae, (d) a mixed phase of lamellae and vesicles, (e) vesicles or (f) precipitate on increasing the PPhA target DP.

this formulation providing significantly better control over the molecular weight distribution; M_w/M_n values range from 1.37 to 1.53 in all cases. Nevertheless, the GPC curve for each copolymer contained a high molecular weight shoulder (see Fig. 6). DLS and TEM studies confirmed that the expected evolution in copolymer morphology occurred on varying the target DP for the structure-directing PPhA block. Thus, the PLA_{14}-$PPhA_{55}$ dispersion was a transparent free-flowing fluid. This is consistent with the formation of spheres, which were found to be approximately 32 nm and relatively uniform in size, as judged by DLS and TEM studies respectively (see Fig. 7a).

An increase in PPhA DP of only ten units produced a turbid free-flowing liquid comprising a mixed phase of spheres and worms (see Fig. 7b). A free-standing transparent gel comprising a pure worm phase was obtained when targeting a PPhA DP of 80 (see Fig. 7c). Further increasing the core-forming block DP produced a mixed phase of worms and vesicles for PLA_{14}-$PPhA_{119}$ (see Fig. 7d), while TEM studies confirmed the existence of a pure vesicle phase for a PPhA DP of 127 (see Fig. 7e).

Open Access Article. Published on 25 July 2017. Downloaded on 3/28/2024 2:51:24 PM.
This article is licensed under a Creative Commons Attribution 3.0 Unported Licence.

Table 3 Summary of monomer conversions, GPC molecular weight data, DLS particle diameters, and copolymer morphologies obtained for a series of PLA_{14}-$PPhA_x$ diblock copolymers synthesized *via* RAFT dispersion polymerization in *n*-heptane at 80 °C[a]

Entry no.	Target diblock composition	Monomer conversion[b]/%	GPC data[c] M_n	GPC data[c] M_w/M_n	DLS diameter[d]/nm	TEM morphology
1	PLA_{14}-$PPhA_{55}$	>99	11 300	1.42	32 (0.10)	Spheres
2	PLA_{14}-$PPhA_{65}$	>99	13 000	1.40	75 (0.15)	Spheres + worms
3	PLA_{14}-$PPhA_{80}$	>99	14 600	1.37	381 (0.49)	Worms
4	PLA_{14}-$PPhA_{120}$	99	18 300	1.40	904 (0.94)	Worms + vesicles
5	PLA_{14}-$PPhA_{130}$	98	20 800	1.53	244 (0.32)	Vesicles

[a] Conditions: [macro-CTA] : [initiator] molar ratio = 5.0; copolymer concentration = 25% w/w. [b] Monomer conversion determined by ^{1}H NMR spectroscopy in $CDCl_3$. [c] Determined by THF GPC (refractive index detector, calibrated with poly(methyl methacrylate) standards). [d] Intensity-average diameters were calculated using cumulants analysis software provided by the manufacturer (Malvern Instruments, UK). The numbers in brackets denote the polydispersity in the particle diameter.

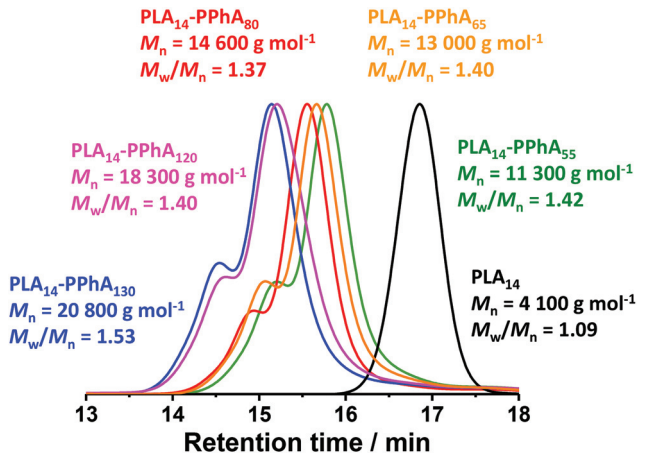


Fig. 6 THF GPC curves obtained for a series of PLA_{14}-$PPhA_x$ diblock copolymers prepared at 25% w/w solids *via* RAFT dispersion polymerization of PhA in *n*-heptane at 80 °C (see Table 3). Molecular weight data are expressed relative to a series of near-monodisperse poly(methyl methacrylate) calibration standards.

Comparing these three PhA-based PISA formulations (see Tables 1–3), significantly higher dispersities are obtained for RAFT aqueous emulsion polymerization at 30 °C compared to the two RAFT dispersion polymerizations conducted at 70 or 80 °C. Similarly broad molecular weight distributions have been reported by other workers for all-acrylic RAFT aqueous emulsion formulation.[60,61] In contrast, significantly lower dispersities (M_w/M_n < 1.30) have been achieved for certain low-temperature RAFT *dispersion* polymerization formulations conducted in either water[65] or ethanol/water mixtures.[67] We postulate that the relatively high dispersities associated with RAFT aqueous emulsion polymerization may be related to stronger partitioning of unreacted monomer within the growing sterically-stabilized nanoparticles. This higher local monomer concentration is consistent with the significantly faster rate of polymerization observed for such PISA formulations relative to RAFT dispersion polymerizations. According to Lovell and co-workers, such a rate enhancement is likely to favor a higher degree of branching *via* chain transfer to polymer.[58]

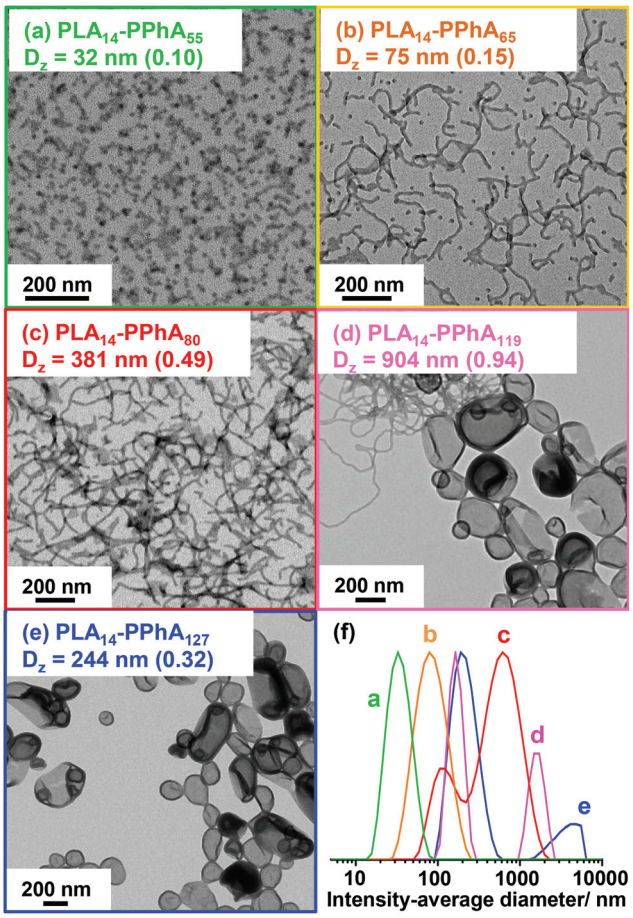


Fig. 7 TEM images and corresponding DLS intensity-average diameters (polydispersity index shown in parentheses) obtained for a series of PLA_{14}-$PPhA_x$ diblock copolymers prepared at 25% w/w solids *via* RAFT dispersion polymerization of phenyl acrylate in *n*-heptane at 80 °C. Increasing the target DP of the structure-directing PPhA block leads to a gradual evolution in copolymer morphology from (a) pure spheres, (b) spheres and worms, (c) worms, (d) worms and vesicles and (e) pure vesicles. (f) The corresponding DLS intensity-average size distributions obtained for these copolymer dispersions.

This journal is © The Royal Society of Chemistry 2017

Open Access Article. Published on 25 July 2017. Downloaded on 3/28/2024 2:51:24 PM.
This article is licensed under a Creative Commons Attribution 3.0 Unported Licence.

To examine this hypothesis, the following control experiments were performed. The $PDMAC_{53}$ macro-CTA was used to polymerize phenyl acrylate *via* RAFT *solution* polymerization in DMF at 30 °C (see ESI† for the precise synthetic protocol and associated characterization data). Three different DPs were targeted for the PPhA core-forming block: 50, 100 and 150. Thus these diblock compositions correspond to entries 1–3 in Table 1. In each case, high PhA conversions (>96%) were achieved after approximately 16 h at 30 °C. DMF GPC analyses indicated high blocking efficiencies and significantly narrower MWDs ($M_w/M_n \leq 1.26$) for all three diblock copolymers. These additional experiments confirm that the $PDMAC_{53}$ macro-CTA has a relatively high end-group fidelity and hence indicate that the problem of high dispersity is instead intimately related to the heterogeneous nature of these PISA formulations. This is consistent with our hypothesis that chain transfer to polymer becomes much more likely within monomer-swollen particles.

Conclusions

Phenyl acrylate is a useful model monomer for conducting fundamental studies focused on acrylic-based PISA formulations. Unlike the vast majority of acrylic polymers, the T_g of poly(phenyl acrylate) is sufficiently high (50 °C) to allow morphological studies to be conducted using conventional TEM, rather than cryo-TEM. Accordingly, phenyl acrylate has been employed to generate the structure-directing solvophobic block in RAFT aqueous emulsion polymerization, RAFT alcoholic dispersion polymerization and RAFT *n*-alkane dispersion polymerization. In the former case, only kinetically-trapped sterically-stabilized spheres could be obtained; this morphological limitation is often reported in the literature and remains poorly understood. In contrast, RAFT dispersion polymerization in either ethanol or *n*-heptane yielded the expected range of copolymer morphologies, depending on the relative volume fractions of the soluble and insoluble blocks. In each case high-quality images could be obtained by TEM. Final monomer conversions were invariably high (>98%) for these PISA syntheses, but GPC analyses indicated relatively broad molecular weight distributions, particularly for RAFT aqueous emulsion polymerization. This is believed to be the result of chain transfer to polymer, which is a well-known side reaction for the polymerization of acrylic monomers when employing either conventional free radical polymerization or pseudo-living radical polymerization techniques such as RAFT. Nevertheless, such branching is no barrier to the convenient formation of well-defined sterically-stabilized diblock copolymer nanoparticles at high solids. In summary, phenyl acrylate is a versatile monomer in the context of fundamental PISA research, which has been hitherto mainly focused on methacrylic monomers or styrene.

Conflict of interest

The authors declare no competing financial interest.

Acknowledgements

EPSRC is thanked for a Platform grant (EP/J007846) and the European Research Council is acknowledged for a five-year Advanced Investigator grant (PISA 320372).

Notes and references

1 B. M. Discher, Y. Won, D. S. Ege, J. C.-M. Lee, F. S. Bates, D. E. Discher and D. A. Hammer, *Science*, 1999, **284**, 1143–1146.
2 D. E. Discher and A. Eisenberg, *Science*, 2002, **297**, 967–973.
3 L. Zhang and A. Eisenberg, *Science*, 1995, **268**, 1728–1731.
4 L. Zhang and A. Eisenberg, *J. Am. Chem. Soc.*, 1996, **118**, 3168–3181.
5 Y. Mai and A. Eisenberg, *Chem. Soc. Rev.*, 2012, **41**, 5969.
6 S. Jain and F. S. Bates, *Macromolecules*, 2004, **37**, 1511–1523.
7 R. Xu, M. A. Winnik, F. R. Hallett, G. Riess and M. D. Croucher, *Macromolecules*, 1991, **24**, 87–93.
8 Y. Won, *Science*, 1999, **283**, 960–963.
9 C. Booth and D. Attwood, *Macromol. Rapid Commun.*, 2000, **21**, 501–527.
10 J. N. Israelachvili, D. J. Mitchell and B. W. Ninham, *J. Chem. Soc., Faraday Trans. 2*, 1976, **72**, 1525–1568.
11 A. Blanazs, S. P. Armes and A. J. Ryan, *Macromol. Rapid Commun.*, 2009, **30**, 267–277.
12 C. J. Hawker, A. W. Bosman and E. Harth, *Chem. Rev.*, 2001, **101**, 3661–3688.
13 M. Kato, M. Kamigaito, M. Sawamoto and T. Higashimura, *Macromolecules*, 1996, **28**, 1721–1723.
14 J. S. Wang and K. Matyjaszewski, *J. Am. Chem. Soc.*, 1995, **117**, 5614–5615.
15 J. Chiefari, Y. K. B. Chong, F. Ercole, J. Krstina, J. Jeffery, T. P. T. Le, R. T. A. Mayadunne, G. F. Meijs, C. L. Moad, G. Moad, E. Rizzardo and S. H. Thang, *Macromolecules*, 1998, **31**, 5559–5562.
16 N. J. Warren and S. P. Armes, *J. Am. Chem. Soc.*, 2014, **136**, 10174–10185.
17 M. J. Derry, L. A. Fielding and S. P. Armes, *Prog. Polym. Sci.*, 2016, **52**, 1–18.
18 S. L. Canning, G. N. Smith and S. P. Armes, *Macromolecules*, 2016, **49**, 1985–2001.
19 B. Charleux, G. Delaittre, J. Rieger and F. D'Agosto, *Macromolecules*, 2012, **45**, 6753–6765.
20 J. Rieger, *Macromol. Rapid Commun.*, 2015, **36**, 1458–1471.
21 J.-T. Sun, C.-Y. Hong and C.-Y. Pan, *Polym. Chem.*, 2013, **4**, 873–881.
22 J.-T. Sun, C.-Y. Hong and C.-Y. Pan, *Soft Matter*, 2012, **8**, 7753–7767.
23 N. J. Warren, O. O. Mykhaylyk, D. Mahmood, A. J. Ryan and S. P. Armes, *J. Am. Chem. Soc.*, 2014, **136**, 1023–1033.
24 S. Sugihara, A. Blanazs, S. P. Armes, A. J. Ryan and A. L. Lewis, *J. Am. Chem. Soc.*, 2011, **133**, 15707–15713.

Open Access Article. Published on 25 July 2017. Downloaded on 3/28/2024 2:51:24 PM.
This article is licensed under a Creative Commons Attribution 3.0 Unported Licence.

25 A. Blanazs, A. J. Ryan and S. P. Armes, *Macromolecules*, 2012, **45**, 5099–5107.
26 P. Yang, L. P. D. Ratcliffe and S. P. Armes, *Macromolecules*, 2013, **46**, 8545–8556.
27 N. J. Warren, O. O. Mykhaylyk, A. J. Ryan, M. Williams, T. Doussineau, P. Dugourd, R. Antoine, G. Portale and S. P. Armes, *J. Am. Chem. Soc.*, 2015, **137**, 1929–1937.
28 L. P. D. Ratcliffe, A. J. Ryan and S. P. Armes, *Macromolecules*, 2013, **46**, 769–777.
29 M. Williams, N. J. W. Penfold, J. R. Lovett, N. J. Warren, C. W. I. Douglas, N. Doroshenko, P. Verstraete, J. Smets and S. P. Armes, *Polym. Chem.*, 2016, **7**, 3864–3873.
30 S. J. Byard, M. Williams, B. E. Mckenzie, A. Blanazs and S. P. Armes, *Macromolecules*, 2017, **50**, 1482–1493.
31 W. Zhou, Q. Qu, Y. Xu and Z. An, *ACS Macro Lett.*, 2015, **4**, 495–499.
32 J. Tan, H. Sun, M. Yu, B. S. Sumerlin and L. Zhang, *ACS Macro Lett.*, 2015, **4**, 1249–1253.
33 M. Semsarilar, E. R. Jones, A. Blanazs and S. P. Armes, *Adv. Mater.*, 2012, **24**, 3378–3382.
34 E. R. Jones, M. Semsarilar, A. Blanazs and S. P. Armes, *Macromolecules*, 2012, **45**, 5091–5098.
35 M. Semsarilar, V. Ladmiral, A. Blanazs and S. P. Armes, *Polym. Chem.*, 2014, **5**, 3466–3475.
36 M. Semsarilar, N. J. W. Penfold, E. R. Jones and S. P. Armes, *Polym. Chem.*, 2015, **6**, 1751–1757.
37 W. Zhao, G. Gody, S. Dong, P. B. Zetterlund and S. Perrier, *Polym. Chem.*, 2014, **5**, 6990–7003.
38 X. Zhang, J. Rieger and B. Charleux, *Polym. Chem.*, 2012, **3**, 1502–1509.
39 W. M. Wan and C. Y. Pan, *Macromolecules*, 2010, **43**, 2672–2675.
40 W. M. Wan, X. L. Sun and C. Y. Pan, *Macromol. Rapid Commun.*, 2010, **31**, 399–404.
41 L. A. Fielding, M. J. Derry, V. Ladmiral, J. Rosselgong, A. M. Rodrigues, L. P. D. Ratcliffe, S. Sugihara and S. P. Armes, *Chem. Sci.*, 2013, **4**, 2081–2087.
42 M. J. Derry, L. A. Fielding and S. P. Armes, *Polym. Chem.*, 2015, **6**, 3054–3062.
43 A. P. Lopez-Oliva, N. J. Warren, A. Rajkumar, O. O. Mykhaylyk, M. J. Derry, K. E. B. Doncom, M. J. Rymaruk and S. P. Armes, *Macromolecules*, 2015, **48**, 3547–3555.
44 L. A. Fielding, J. A. Lane, M. J. Derry, O. O. Mykhaylyk and S. P. Armes, *J. Am. Chem. Soc.*, 2014, **136**, 5790–5798.
45 L. Houillot, C. Bui, M. Save, B. Charleux, C. Farcet, C. Moire, J.-A. Raust and I. Rodriguez, *Macromolecules*, 2007, **40**, 6500–6509.
46 V. J. Cunningham, A. M. Alswieleh, K. L. Thompson, M. Williams, G. J. Leggett, S. P. Armes and O. M. Musa, *Macromolecules*, 2014, **47**, 5613–5623.
47 A. A. Cockram, T. J. Neal, M. J. Derry, O. O. Mykhaylyk, N. S. J. Williams, M. W. Murray, S. N. Emmett and S. P. Armes, *Macromolecules*, 2017, **50**, 796–802.
48 J. Rieger, W. Zhang, F. Stoffelbach and B. Charleux, *Macromolecules*, 2010, **43**, 6302–6310.
49 W. Zhang, F. D'Agosto, O. Boyron, J. Rieger and B. Charleux, *Macromolecules*, 2011, **44**, 7584–7593.
50 S. Boissé, J. Rieger, G. Pembouong, P. Beaunier and B. Charleux, *J. Polym. Sci., Part A: Polym. Chem.*, 2011, **49**, 3346–3354.
51 W. Zhang, F. D'Agosto, O. Boyron, J. Rieger and B. Charleux, *Macromolecules*, 2012, **45**, 4075–4084.
52 W. Zhang, F. D'Agosto, P. Y. Dugas, J. Rieger and B. Charleux, *Polym.*, 2013, **54**, 2011–2019.
53 P. A. Steward, J. Hearn and M. C. Wilkinson, *Adv. Colloid Interface Sci.*, 2000, **86**, 195–267.
54 Z. Czech, *Polym. Int.*, 2003, **52**, 347–357.
55 N. M. Ahmad, D. J. Britton, F. Heatley and P. A. Lovell, *Macromol. Symp.*, 1999, **143**, 231–241.
56 F. Heatley, P. A. Lovell and T. Yamashita, *Macromolecules*, 1998, **31**, 2828–2837.
57 C. Plessis, G. Arzamendi, J. M. Alberdi, M. Agnely, J. R. Leiza and J. M. Asua, *Macromolecules*, 2001, **34**, 6138–6143.
58 N. M. Ahmad, B. Charleux, C. Farcet, C. J. Ferguson, S. G. Gaynor, B. S. Hawkett, F. Heatley, B. Klumperman, D. Konkolewicz, P. A. Lovell, K. Matyjaszewski and R. Venkatesh, *Macromol. Rapid Commun.*, 2009, **30**, 2002–2021.
59 Y. Reyes and J. M. Asua, *Macromol. Rapid Commun.*, 2011, **32**, 63–67.
60 M. Chenal, L. Bouteiller and J. Rieger, *Polym. Chem.*, 2013, **4**, 752–762.
61 C. J. Ferguson, R. J. Hughes, D. Nguyen, B. T. T. Pham, R. G. Gilbert, A. K. Serelis, C. H. Such and B. S. Hawkett, *Macromolecules*, 2005, **38**, 2191–2204.
62 X. Zhang, S. Boissé, C. Bui, P.-A. Albouy, A. Brûlet, M.-H. Li, J. Rieger and B. Charleux, *Soft Matter*, 2012, **8**, 1130–1141.
63 L. Houillot, C. Bui, C. Farcet, C. Moire, J. A. Raust, H. Pasch, M. Save and B. Charleux, *ACS Appl. Mater. Interfaces*, 2010, **2**, 434–442.
64 J. Zhou, R. He and J. Ma, *Polymers*, 2016, **8**, 207.
65 G. Liu, Q. Qiu, W. Shen and Z. An, *Macromolecules*, 2011, **44**, 5237–5245.
66 L. P. D. Ratcliffe, B. E. McKenzie, G. M. D. Le Bouëdec, C. N. Williams, S. L. Brown and S. P. Armes, *Macromolecules*, 2015, **48**, 8594–8607.
67 J. Tan, C. Huang, D. Liu, X. Zhang, Y. Bai and L. Zhang, *ACS Macro Lett.*, 2016, **5**, 894–899.
68 R. Diaz-Calleja, E. Riande and J. San Román, *Macromolecules*, 1991, **24**, 1854–1858.
69 *Polymer Handbook*, ed. J. Brandrup and E. H. Immergut, Wiley & Sons, 1975.
70 A. Blanazs, J. Madsen, G. Battaglia, A. J. Ryan and S. P. Armes, *J. Am. Chem. Soc.*, 2011, **133**, 16581–16587.
71 C. J. Ferguson, R. J. Hughes, B. T. T. Pham, B. S. Hawkett, R. G. Gilbert, A. K. Serelis and C. H. Such, *Macromolecules*, 2002, **35**, 9243–9245.
72 N. P. Truong, M. V. Dussert, M. R. Whittaker, J. F. Quinn and T. P. Davis, *Polym. Chem.*, 2015, **6**, 3865–3874.

This journal is © The Royal Society of Chemistry 2017

Open Access Article. Published on 25 July 2017. Downloaded on 3/28/2024 2:51:24 PM.
This article is licensed under a Creative Commons Attribution 3.0 Unported Licence.

73 L. Carlsson, A. Fall, I. Chaduc, L. Wagberg, B. Charleux, E. Malmstrom, F. D'Agosto, M. Lansalot and A. Carlmark, *Polym. Chem.*, 2014, **5**, 6076–6086.
74 Y. Ning, L. A. Fielding, T. S. Andrews, D. Growney and S. P. Armes, *Nanoscale*, 2015, **7**, 6691–6702.
75 L. Guo, Y. Jiang, T. Qiu, Y. Meng and X. Li, *Polym.*, 2014, **55**, 4601–4610.
76 J. Rieger, G. Osterwinter, C. Bui, F. Stoffelbach and B. Charleux, *Macromolecules*, 2009, **42**, 5518–5525.
77 X. Zhang, S. Boissé, W. Zhang, P. Beaunier, F. D'Agosto, J. Rieger and B. Charleux, *Macromolecules*, 2011, **44**, 4149–4158.
78 S. Boissé, J. Rieger, K. Belal, A. Di-Cicco, P. Beaunier, M.-H. Li and B. Charleux, *Chem. Commun.*, 2010, **46**, 1950–1952.
79 M. Semsarilar, V. Ladmiral, A. Blanazs and S. P. Armes, *Langmuir*, 2013, **29**, 7416–7424.
80 M. Semsarilar, V. Ladmiral, A. Blanazs and S. P. Armes, *Langmuir*, 2012, **28**, 914–922.
81 K. E. B. Doncom, N. J. Warren and S. P. Armes, *Polym. Chem.*, 2015, **6**, 7264–7273.
82 P. Yang, O. O. Mykhaylyk, E. R. Jones and S. P. Armes, *Macromolecules*, 2016, **49**, 6731–6742.
83 W. Cai, W. Wan, C. Hong, C. Huang and C. Pan, *Soft Matter*, 2010, **6**, 5554–5561.
84 J. R. Lovett, N. J. Warren, L. P. D. Ratcliffe, M. K. Kocik and S. P. Armes, *Angew. Chem.*, 2015, **127**, 1295–1299.
85 M. J. Derry, L. A. Fielding, N. J. Warren, C. J. Mable, A. J. Smith, O. O. Mykhaylyk and S. P. Armes, *Chem. Sci.*, 2016, **7**, 5078–5090.